Molecular Simulation of Multicomponent Reaction and Phase Equilibria in MTBE Ternary System

Martin Lísal
E. Hála Laboratory of Thermodynamics, Institute of Chemical Process Fundamentals, Academy of Sciences, 165 02 Prague 6, Czech Republic

William R. Smith
Dept. of Mathematics and Statistics, and School of Engineering, College of Physical and Engineering Science, University of Guelph, Guelph, Ontario N1G 2W1, Canada

Ivo Nezbeda
E. Hála Laboratory of Thermodynamics, Institute of Chemical Process Fundamentals, Academy of Sciences, 165 02 Prague 6, Czech Republic, and Dept. of Physics, J. E. Purkyně University, 400 96 Ústí n. Lab., Czech Republic

Reaction and phase equilibria in the isobutene + methanol + MTBE ternary system were studied using the reaction-ensemble Monte Carlo (REMC) simulation method. The system was modeled at the molecular level by an OPLS force field. No adjustable binary cross-interaction parameters or mixture data of any kind were used in the simulation model, and only vapor-pressure data for the pure components was required as input. The REMC method also computes excess internal energies and molar volumes as a biproduct of the simulations. Both the nonreacting and reacting ternary systems were considered over the temperature range of practical interest at 5 bar. Results are compared with the calculations using two conventional thermodynamic approaches: the Wilson and UNIFAC free-energy models for the liquid phase, together with a truncated virial equation of state for the gas phase in both cases. Computer simulation results were similar to those of the thermodynamic approaches, and they are arguably more accurate.

Introduction

The accurate prediction of reaction and phase equilibria for complex chemical systems is an important problem in chemical engineering. There are two general approaches to the solution of this problem. The conventional engineering approach utilizes a semiempirical chemical-potential model and equation-of-state (EOS) expressions to model the system properties over the complete composition range; the mixture properties are then calculated by minimizing an appropriate thermodynamic potential function over the composition variables (such as Smith and Missen, 1991). Methods in this class of approaches include the UNIFAC (and other group-contribution approaches), Wilson, and NRTL free-energy models (Reid et al., 1987; Walas, 1985), and various EOS models. All such methods utilize, as input information, experimental data for the underlying pure components of the mixture; they also require binary mixture data of some type.

The other approach to the calculation of phase and reaction equilibria involves modeling the intermolecular interactions between the constituent molecules of the system and the use of computer simulation techniques, based on either the Gibbs ensemble Monte Carlo (GEMC) method (Panagiotopoulos, 1992; Panagiotopoulos et al., 1988) for phase-equilibrium calculations, or the reaction-ensemble Monte Carlo (REMC) technique (Smith and Tříska, 1994; Lísal et al., 1999a) for the calculation of the reaction and phase equilibrium.

Correspondence concerning this article should be addressed to M. Lísal.

The former methods are well-established chemical engineering tools. The GEMC method has not been considered competitive with the classic approach in its predictive accuracy of *P-T-x* phase-equilibrium properties (where P is the system pressure, T the temperature, and x denotes a general set of phase compositions), primarily as a result of the fact that P is very sensitive to the details of the underlying intermolecular potential model. Recently (Lísal et al., 1999b), we have developed the reaction Gibbs ensemble Monte Carlo (RGEMC) method, whose predictive accuracy for phase-equilibrium calculations is competitive with that of the classic approaches. The purpose of this article is to apply the REMC and RGEMC approaches to a complex system of industrial importance that exhibits combined reaction and phase-equilibrium behavior.

Methyl-*tert*-butyl ether (MTBE) is an important compound used as an antiknock agent in unleaded gasoline. It is synthesized from the reaction between isobutene and methanol. This ternary reacting system requires a catalyst, and is typically augmented by inert C_4 (such as *n*-butane or 1-butene). The inerts and reaction product are separated by distillation; the combined reaction and phase-equilibrium phenomenon is known as reactive distillation (DeGarmo et al., 1992).

An important aspect of modeling the reactive distillation process is the calculation of the simultaneous chemical and vapor–liquid equilibrium. The existence of a chemical reaction in a system significantly affects the structure and properties of the underlying phase diagrams. For example, the nonreacting MTBE ternary system has two minimum-boiling binary azeotropes, one involving methanol and MTBE, the other involving methanol and isobutene. The interaction of these two azeotropes divides the composition triangle into two simple distillation regions. However, in the reacting MTBE ternary system, both binary azeotropes disappear (Doherty and Buzad, 1992).

Experimental studies concerning the MTBE system are mostly limited to the binaries involved [for references, see Wichterle et al. (1996) and Marsh et al. (1999)]; we are not aware of any experimental data in the open literature concerning the MTBE reactive system. In the nonreacting case, some vapor–liquid equilibrium (VLE) data of the isobutene + methanol + MTBE ternary system was measured by Vetere et al. (1993). They also considered modeling the system using the UNIFAC free-energy model and the Vetere EOS (Vetere, 1991); they found that these gave reasonable, but not quantitatively accurate, predictions. They also considered correlating the data using the NRTL free-energy model.

Theoretical studies modeling the MTBE reactive system, primarily by Doherty and coworkers, can be divided into two groups according to the methods employed: one used the Wilson free-energy model together with an ideal-gas description of the vapor phase (Barbosa and Doherty, 1988; Ung and Doherty, 1995a), and the other utilized residue curve maps (Ung and Doherty, 1995b; Jacobs and Krishna, 1993). These works investigated interesting qualitative features of the reactive system, but did not make comparisons with any experimental data.

In our earlier article (Lísal et al., 1999b), we considered the prediction of the VLE for the underlying binary systems of the MTBE ternary system, obtaining excellent results using the RGEMC method. In the present article, we study the simultaneous chemical and vapor–liquid equilibrium of the MTBE ternary system. We consider predictions of the system behavior in both the nonreacting and reacting cases, at a typical pressure and over a temperature range of practical interest ($P = 5$ bar, $\{355\ \text{K} \le T \le 370\ \text{K}\}$). We compute the reaction and phase-equilibrium properties results for the system; we use the RGEMC method for the nonreacting system, and the REMC method for the reacting system. We compare these results with our predictions calculated using the Wilson and the UNIFAC free-energy models for the liquid, together with a truncated virial EOS for the gas phase (referred to herein as the Wilson + B-EOS and UNIFAC + B-EOS approximations, respectively).

In the next section, we summarize the thermodynamic modeling of the MTBE reaction system using EOS and free-energy models. In the subsequent section, we describe the computational details of the REMC approach. We then present and discuss our results, followed by conclusions.

Thermodynamic Modeling of the MTBE System

The equilibrium compositions of vapor (y) and liquid (x) at specified temperature T and pressure P in the MTBE reactive system are determined by solving the conditions for chemical and vapor–liquid equilibrium simultaneously. The relevant conditions are the equilibrium condition for the reaction:

$$i\text{-}C_4H_8\ (1) + \text{MeOH}\ (2) = \text{MTBE}\ (3) \qquad (1)$$

and the phase equilibrium conditions:

$$\mu_i^g = \mu_i^\ell \qquad i = 1, \ldots, 3. \qquad (2)$$

The reaction equilibrium condition can be expressed in terms of the chemical potentials μ_i in either the vapor (g) or the liquid (ℓ) phase as

$$\sum_{j=1}^{3} \nu_i \mu_i^\phi = 0, \qquad (3)$$

where ϕ refers to the phase. The stoichiometric coefficients corresponding to Eq. 1 are, respectively, $\nu_1 = -1$, $\nu_2 = -1$, and $\nu_3 = 1$ for the three species, and their sum $\bar{\nu} = -1$.

We may express the chemical potentials in the vapor and liquid phases, respectively, as

$$\mu_i^g(T, P, y) = \mu_i^0(T, P^0) + RT \ln y_i \Phi_i(T, P, y) P \qquad (4)$$

$$\mu_i^\ell(T, P, x) = \mu_i(T, P) + RT \ln x_i \gamma_i(T, P, x), \qquad (5)$$

where $\mu_i^0(T, P^0)$ is the standard chemical potential of species i in the ideal-gas state at the system temperature T and a standard-state pressure P^0; R is the universal gas constant ($R = 8.3145\ \text{J}\cdot\text{mol}^{-1}\cdot\text{K}^{-1}$); Φ_i is the fugacity coefficient of species i; and γ_i is the activity coefficient of species i. At low pressures, as is the case considered herein, the difference between $\mu_i(T, P)$ and $\mu_i(T, P_i^{\text{sat}})$ (where P_i^{sat} is the vapor pressure of species i at the temperature T) is negligible, and

we can set

$$\mu_i(T,P) = \mu_i\left(T, P_i^{\text{sat}}\right) \equiv \mu_i^0(T,P^0) + RT\ln\Phi_i^{\text{sat}}\left(T,P_i^{\text{sat}}\right)P_i^{\text{sat}}(T), \quad (6)$$

yielding the phase-equilibrium conditions in the form

$$y_i\Phi_i P = x_i\gamma_i P_i^{\text{sat}}\Phi_i^{\text{sat}} \qquad i=1,\ldots,3. \quad (7)$$

The reaction-equilibrium conditions (Eq. 1), written for the gas and the liquid phases, respectively, are:

$$KP = \frac{y_3}{y_1 y_2}\cdot\frac{\Phi_3}{\Phi_1\Phi_2} \quad (8)$$

$$K = \frac{x_3}{x_1 x_2}\cdot\frac{\gamma_3}{\gamma_1\gamma_2}\cdot\frac{P_3^{\text{sat}}}{P_1^{\text{sat}}P_2^{\text{sat}}}\cdot\frac{\Phi_3^{\text{sat}}}{\Phi_1^{\text{sat}}\Phi_2^{\text{sat}}}, \quad (9)$$

where the equilibrium constant K is defined by

$$K \equiv \exp\left[-\frac{\Delta G^0(T)}{RT}\right] = \exp\left[-\frac{\mu_3^0(T)-\mu_1^0(T)-\mu_2^0(T)}{RT}\right]. \quad (10)$$

The molar standard chemical potentials $\mu_i^0(T,P^0)$ can be expressed as (omitting the dependence on the standard-state pressure, taken to be 1 bar)

$$\mu_i^0(T) = h_i^0(T) - Ts_i^0(T), \quad (11)$$

where the molar enthalpy, $h_i(T)$, and the molar entropy, $s_i^0(T)$, are given by

$$h_i^0(T) = \Delta H_{fi}(T_r) + \int_{T_r}^{T} C_{pi}(T)\,dT \quad (12)$$

$$s_i^0(T) = s_i^0(T_r) + \int_{T_r}^{T}\frac{C_{pi}(T)}{T}\,dT, \quad (13)$$

where $\Delta H_{fi}(T_r)$ is the standard enthalpy of formation of species i at the reference temperature T_r (taken as 298.15 K); $s_i^0(T_r)$ is the conventional absolute entropy of species i at the reference temperature; and $C_{pi}(T)$ is the ideal-gas heat capacity of species i.

Values of $\Delta H_{fi}(T_r)$ and $s_i^0(T_r)$ are conventionally available in tabular form (such as Chase et al., 1985), and $C_{pi}(T)$ are available in terms of polynomials in T (Frenkel et al., 1994). The required data for isobutene, methanol, and MTBE are given in Table 1. From these data, the equilibrium constant K for the MTBE reaction can be expressed in the final form

$$K = \exp\left(-A - \frac{B}{T} - C\ln T - \sum_{i=1}^{4} D_i T^i\right), \quad (14)$$

where $A = 12.800$; $B = -7{,}813.260$; $C = 1.530$; $D_1 = -1.339\times10^{-3}$; $D_2 = -3.343\times10^{-6}$; $D_3 = 3.076\times10^{-9}$; and $D_4 = -8.765\times10^{-13}$. In Figure 1, we compare the equilibrium constant K evaluated using Eq. 14, and using the expression given by Colombo et al. (1983). These workers assumed that $C_{p,i}$ were constant and equal to the values at 298.15 K; hence, our Eq. 14 for K is more precise than that of Colombo et al. (1983), and furthermore, it is applicable over a larger temperature interval. From Figure 1, it is seen that both equilibrium constants differ only marginally for the temperature interval of interest in this article.

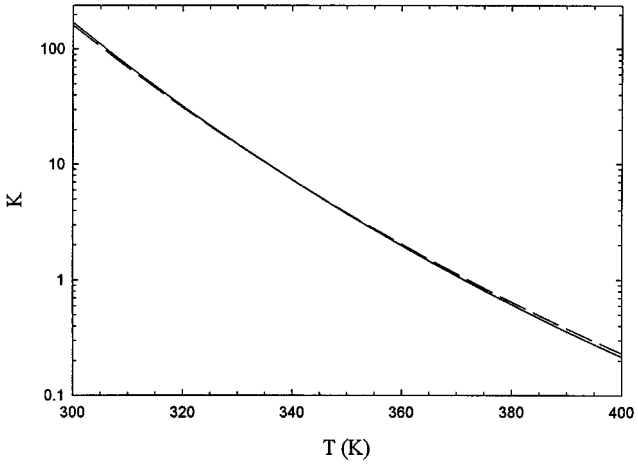

Figure 1. Equilibrium constant *K* for the MTBE reaction as a function of temperature *T*.

The solid line is the calculation of this work, and the dashed line represents K values extracted from Colombo et al. (1983).

The vapor pressures $P_i^{\text{sat}}(T)$ are conveniently correlated using the Antoine equation

$$\ln P_i^{\text{sat}} = A_i + \frac{B_i}{T + C_i} \qquad (\text{bar, K}). \quad (15)$$

The Antoine coefficients are given in Table 2.

Table 1. Thermochemical Data for Isobutene, Methanol, and MTBE*

Component	ΔH_f^0 (J/mol)	S_i^0 (J/mol·K)	a_0/R	$a_1/R\times10^3$ (K^{-1})	$a_2/R\times10^5$ (K^{-2})	$a_3/R\times10^8$ (K^{-3})	$a_4/R\times10^{11}$ (K^{-4})
Isobutene (1)	−16,903.36**	293.21††	3.321††	20.949††	2.313††	−3.949††	1.566††
Methanol (2)	−201,041.2**	239.83††	4.714††	−6.986††	4.211††	−4.443††	1.535††
MTBE (3)	−283,700†	353.05††	6.415††	16.641††	8.530††	−12.083††	4.854††

*$\Delta H_f^0(298.15)$, $S_i^0(298.15)$, and coefficients $a_0, \ldots, a_4$ of the fourth-order polynomial expression for the ideal-gas heat capacity C_p; R is the universal gas constant.
**Data taken from Marsh (1979).
†Data taken from Pedley, (1994).
††Data taken from Frenkel et al. (1994).

Table 2. Coefficients of the Antoine Vapor-Pressure Equation A, B, and C for Isobutene, Methanol, and MTBE from Experiments* and GEMC Simulations**

	Exp.			GEMC		
Component	A	B	C	A	B	C
Isobutene (1)	9.132635	−2,125.74886	−33.160	8.4977389	−1,817.1451	−54.720771
Methanol (2)	11.986965	−3,643.31362	−33.434	10.765146	−3,106.2980	−40.414885
MTBE (3)	9.203235	−2,571.58460	−48.406	10.355395	−3,759.4247	28.103582

*Ung and Doherty (1995a).
**Lísal et al. (1999b).

The combined phase and reaction equilibrium compositions $\{x_1, x_2, x_3, y_1, y_2, y_3\}$ are determined by the simultaneous solution of Eqs. 7 and either Eq. 8 or 9, along with the conditions that the mol fractions add to unity in each phase. We calculated the vapor-phase fugacity coefficients from the virial EOS, truncated at the second virial coefficient (B-EOS) (Smith et al., 1996), and the liquid-phase activity coefficients were calculated by means of either the Wilson (Ung and Doherty, 1995a) or the UNIFAC (Reid et al., 1987) free-energy models. The Wilson and UNIFAC parameters are given in Appendices A and B, respectively.

REMC Simulation Methodology for MTBE System

Phase and reaction equilibrium of the MTBE system at fixed (T, P) requires equilibrium for the "chemical equations":

$$i\text{-}C_4H_8(g) = i\text{-}C_4H_8(\ell) \tag{16}$$

$$CH_3OH(g) = CH_3OH(\ell) \tag{17}$$

$$MTBE(g) = MTBE(\ell) \tag{18}$$

$$i\text{-}C_4H_8 + CH_3OH = MTBE. \tag{19}$$

In Eq. 19, each species may be in either phase. We remark that we have used the convention that a *chemical species* is characterized by both its chemical formula and its phase, enabling the treatment of phase equilibria on exactly the same basis as reaction equilibria (Smith and Missen, 1991). There are four independent stoichiometric reactions for this system, and the preceding equations form a linearly independent set.

The MTBE ternary system was modeled at the molecular level using an OPLS force-field model; for details, see Lísal et al. (1999b). This approach models the force fields between constituent groups of atoms in a molecule, similar in spirit to group-contribution methods in classic thermodynamics. The groups are characterized by pair potentials involving Lennard-Jones, Coulombic pair, and other appropriate terms. We used the OPLS combining rules with no adjustable binary cross-interaction parameters for unlike interaction parameters. In our earlier article (Lísal et al., 1999b), we showed that this approach, in combination with the RGEMC method employed in the present article, gave excellent predictions of the experimental vapor–liquid equilibrium data for the underlying binaries of the MTBE ternary system, including the highly nonideal systems of methanol with isobutene and MTBE.

The vapor and liquid phases were represented in the simulations by two separate boxes: an arbitrary simulation box in the following will be denoted by the symbol α. In the REMC method (Smith and Tříska, 1994; Lísal et al., 1999a), the required conditions of vapor–liquid and reaction equilibrium are ensured by performing a combination of four steps: particle displacements, volume changes to maintain a constant pressure P, interphase particle transfers for the phase equilibria, and reaction moves corresponding to the reaction equilibrium.

The transition probability $k \to l$ for a particle displacement in box α (Allen and Tildesley, 1987) is

$$P_{kl}^{D} = \min\left[1, \exp(-\beta \Delta U_{kl}^{\alpha})\right], \tag{20}$$

and the transition probability $k \to l$ for a volume change of box α (Allen and Tildesley, 1987) is

$$P_{kl}^{V} = \min\left\{1, \exp\left[-\beta \Delta U_{kl}^{\alpha} - \beta P\left(V_l^{\alpha} - V_k^{\alpha}\right) + N^{\alpha} \ln \frac{V_l^{\alpha}}{V_k^{\alpha}}\right]\right\}. \tag{21}$$

In Eqs. 20 and 21, $\Delta U_{kl}^{\alpha} = U_l^{\alpha} - U_k^{\alpha}$ is the change in configurational energy in box α; $\beta = 1/(k_B T)$, k_B is Boltzmann's constant; V^{α} is the volume of box α; and N^{α} is the total number of molecules in box α.

The interphase particle transfers involve choosing the donor and recipient boxes at random, then randomly choosing the particle that is to be transferred from the donor box regardless of its type, and then transferring it to a random position in the recipient box. Using our RGEMC approach (Lísal et al., 1999b), the transition probability $k \to l$ for the transfer of a particle from the liquid box (ℓ) into the vapor box (g) is

$$P_{kl}^{\ell \to g} = \min\left\{1, \Gamma_i \exp\left[-\beta \Delta U_{kl}^{\ell} - \beta \Delta U_{kl}^{g} + \ln \frac{N^{\ell} V^{g}}{(N^{g}+1) V^{\ell}}\right]\right\}, \tag{22}$$

and similarly the transition probability $k \to l$ for the transfer of a particle from the vapor box (g) into the liquid box (ℓ) is

$$P_{kl}^{g \to \ell} = \min\left\{1, \frac{1}{\Gamma_i} \exp\left[-\beta \Delta U_{kl}^{g} - \beta \Delta U_{kl}^{\ell} + \ln \frac{N^{g} V^{\ell}}{(N^{\ell}+1) V^{g}}\right]\right\}, \tag{23}$$

where Γ_i is the pseudo-ideal-gas driving term for a phase equilibrium reaction i [Eqs. 16–18], given by

$$\Gamma_i = \frac{P_{i,\mathrm{exp}}^{\mathrm{sat}}(T)}{P_{i,\mathrm{simul}}^{\mathrm{sat}}(T)}, \tag{24}$$

where $P^{\text{sat}}_{i,\text{exp}}(T)$ and $P^{\text{sat}}_{i,\text{simul}}(T)$ are the experimental and simulation vapor pressures of the transferred species i, respectively. Data for $P^{\text{sat}}_{i,\text{exp}}$ and $P^{\text{sat}}_{i,\text{simul}}$, in terms of the Antoine equation (Eq. 15), is given in Table 2.

Reaction moves for the MTBE reaction (Eq. 19) need be carried out only in one phase box for the system at hand, since Eqs. 16–19 form a maximal linearly independent set of chemical equations. For convenience, we performed these moves in the vapor box; however, other strategies are possible, which will affect the convergence (but not the final results) of the method. The reaction moves were carried out in forward and reverse directions according to a preset probability of 0.5. In the forward direction, an $i-C_4H_8$ molecule and a CH_3OH molecule (reactants) are chosen at random, and an attempt is made to simultaneously replace the $i-C_4H_8$ molecule by an MTBE molecule (product) and delete the CH_3OH molecule from the fluid. The transition probability $k \rightarrow l$ for the forward reaction moves (Smith and Tříska, 1994), is

$$P^{FR}_{kl} = \min\left[1, \frac{\Gamma}{V^{\alpha}} \frac{N^{\alpha}_{i-C_4H_8} N^{\alpha}_{CH_3OH}}{N^{\alpha}_{MTBE}+1} \exp\left(-\beta \Delta U^{\alpha}_{kl}\right)\right]. \quad (25)$$

Similarly, in the reverse direction, an MTBE molecule (product) is chosen at random, and an attempt is made to simultaneously replace the MTBE molecule by an $i-C_4H_8$ molecule (reactant) and to randomly insert a CH_3OH molecule (reactant) into the fluid. This transition probability $k \rightarrow l$ for the reverse reaction moves (Smith and Tříska, 1994), is

$$P^{RR}_{kl} = \min\left[1, \frac{V^{\alpha}}{\Gamma} \frac{N^{\alpha}_{MTBE}}{\left(N^{\alpha}_{i-C_4H_8}+1\right)\left(N^{\alpha}_{CH_3OH}+1\right)} \exp\left(-\beta \Delta U^{\alpha}_{kl}\right)\right]. \quad (26)$$

In Eqs. 25 and 26, $N^{\alpha}_{i-C_4H_8}$, $N^{\alpha}_{CH_3OH}$, and N^{α}_{MTBE} are the numbers of molecules of $i-C_4H_8$, CH_3OH, and MTBE in box α, respectively.

The ideal-gas driving term Γ for the MTBE reaction is given by (Smith and Tříska, 1994)

$$\Gamma \equiv \exp\left(-\frac{\Delta G^0}{RT}\right)\left(\frac{P^0}{k_B T}\right)^{\bar{\nu}} = K \frac{k_B T}{P^0}. \quad (27)$$

We used $N = 512$ particles in cubic simulation boxes, the minimum image convention, periodic boundary conditions, and cutoff radius equal to half the box length. The Lennard-Jones long-range correction for the configurational energy was included (Allen and Tildesley, 1987), assuming that the radial distribution functions are unity beyond the cutoff radius. We treated the Coulombic long-range interactions by the reaction-field method (Jedlovszky and Pálinkás, 1995) with the reaction-field dielectric constant set to infinity. The REMC simulations were organized in cycles as follows. Each cycle consisted of four steps: n_D translation and rotational moves; n_V volume moves; n_T particle transfers; and n_ξ forward and reverse reaction moves. The four types of moves were selected at random, with fixed probabilities chosen so that the ratio $n_D : n_V : n_T : n_\xi$ in the cycle was $N : 2 : 5{,}000 : N$. Acceptance ratios for translation and rotational moves, and for volume changes, were adjusted to approximately 30%. After an initial equilibration period of $1-2\times10^4$ cycles, we generated (depending on the thermodynamic conditions) between $0.5-1\times10^5$ cycles to accumulate averages of the desired quantities. The precision of the simulation data was obtained using block averages, with 500 cycles per block. In addition to ensemble averages of the quantities of direct interest, we also monitored convergence profiles of the thermodynamic quantities, in order to keep the development of the system under control (Nezbeda and Kolafa, 1995).

Results and Discussion

We studied the nonreacting and the reacting MTBE ternary system at the pressure 5 bar; the temperature interval for the existence of simultaneous reaction and vapor–liquid equilibrium at this pressure corresponds to the temperature interval of practical interest (DeGarmo et al., 1992). In Table 3, we summarize, for convenience, several pure-component properties for the species involved in the MTBE ternary system.

Nonreacting MTBE ternary system

We performed RGEMC simulations at constant P (NPT RGEMC) for the VLE (the reaction moves were switched off in the simulations) of the MTBE ternary system at $T = 375$ K and 360 K, and $P = 5$ bar. Our new NPT RGEMC simulation data for this system are given in Tables 4 and 5. We note that our simulation results include values of the excess internal energy U^e and the molar volumes V_m. These are easily computed byproducts of the simulations. In Figure 2, we show intersections of planes of constant T with the $\{T, z_1, z_2\}$ isobaric phase-equilibrium surface (where z_i is the mole fractions of species i in the vapor or liquid phase) in the triangular composition simplex at the temperatures and pressure studied, obtained both from our NPT RGEMC simulations and from our calculations using the Wilson + B-EOS and UNIFAC + B-EOS approximations.

At $T = 375$ K (Figure 2a), the VLE curves split the composition simplex into a large vapor region, and smaller liquid and vapor–liquid regions. There are two vapor–liquid regions located near the pure methanol and the pure MTBE vertexes; this is a consequence of the presence of a minimum-boiling azeotrope in the methanol + MTBE binary system. For the region near pure MTBE, the simulation liquid curve is numerically identical on the scale of the graph to that calculated from the Wilson + B-EOS approximation, and

Table 3. Pure-Component Properties for Isobutene, Methanol, and MTBE*

Component	M (g/mol)	T_c (K)	P_c (bar)	V_c (cm^3/mol)	ω	T_b (K)	T_m (K)
Isobutene (1)	56.1075	417.9	40.0	239	0.1940	266.2	132.7
Methanol (2)	32.0422	512.6	80.9	118	0.5560	337.7	175.5
MTBE (3)	88.1497	496.4	33.7	327	0.2690	328.3	164.5

*M is the molecular weight, T_c is the critical temperature, P_c is the critical pressure, V_c is the critical molar volume, ω is Pitzer's acentric factor, T_b is the normal boiling temperature, and T_m is the melting temperature. Data were taken from Reid et al. (1987) and Lide (1999).

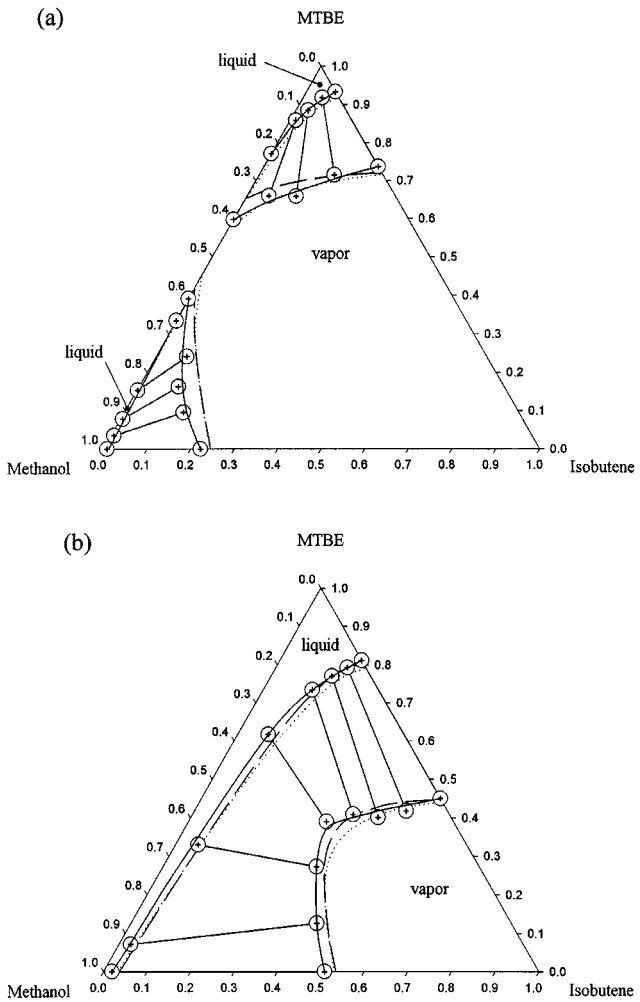

Figure 2. Triangular composition simplexes for vapor–liquid equilibria in the nonreacting isobutene + methanol + MTBE ternary system at the temperatures (a) 375 K and (b) 360 K, and the pressure 5 bar.

Crosses connected by tie-lines indicate the NPT RGEMC simulation results of this work; circles around the crosses denote approximately the statistical uncertainties of the simulation results. The solid lines drawn through the simulation results are guides for the eye only. The dashed and dotted lines represent predictions of this work using the Wilson + B-EOS and UNIFAC + B-EOS approximations, respectively.

Table 4. Vapor–Liquid Equilibrium Data for the MTBE Ternary System at the Temperature 375 K and Pressure 5 bar from the NPT RGEMC Simulations of this Article*

Isobutene (1) + Methanol (2) + MTBE (3); $T = 375$ K, $P = 5$ bar						
	z_1	z_2	z_3	ϕ	U^e (kJ/mol)	V_m (cm^3/mol)
$n_{10} = 0.175$, $n_{20} = 0$, $n_{30} = 0.825$						
g	0.2631_{128}	0	0.7369_{128}	0.558_{39}	-0.85_{13}	$5{,}470_{99}$
ℓ	0.0664_{73}	0	0.9336_{173}	0.442_{39}	-23.44_{31}	130.2_{14}
$n_{10} = 0.110$, $n_{20} = 0.075$, $n_{30} = 0.815$						
g	0.1729_{111}	0.1115_{84}	0.7156_{175}	0.525_{55}	-0.85_{6}	$5{,}535_{132}$
ℓ	0.0438_{79}	0.0375_{66}	0.9187_{114}	0.475_{55}	-23.52_{25}	127.8_{10}
$n_{10} = 0.065$, $n_{20} = 0.150$, $n_{30} = 0.785$						
g	0.1134_{61}	0.2277_{120}	0.6589_{150}	0.451_{30}	-0.93_{14}	$5{,}537_{131}$
ℓ	0.0279_{43}	0.0870_{89}	0.8851_{100}	0.549_{30}	-23.59_{29}	124.5_{11}
$n_{10} = 0.035$, $n_{20} = 0.225$, $n_{30} = 0.740$						
g	0.0505_{21}	0.2897_{105}	0.6598_{111}	0.593_{29}	-1.03_{13}	$5{,}554_{146}$
ℓ	0.0128_{26}	0.1286_{180}	0.8586_{190}	0.407_{29}	-23.78_{26}	121.4_{17}
$n_{10} = 0$, $n_{20} = 0.325$, $n_{30} = 0.675$						
g	0	0.4027_{183}	0.5973_{183}	0.558_{22}	-1.12_{22}	$5{,}579_{167}$
ℓ	0	0.2288_{230}	0.7712_{230}	0.442_{22}	-24.26_{40}	113.2_{23}
$n_{10} = 0$, $n_{20} = 0.615$, $n_{30} = 0.385$						
g	0	0.6088_{178}	0.3912_{178}	0.899_{30}	-1.37_{17}	$5{,}501_{209}$
ℓ	0	0.6653_{214}	0.3347_{214}	0.101_{30}	-23.62_{43}	82.99_{13}
$n_{10} = 0.060$, $n_{20} = 0.715$, $n_{30} = 0.225$						
g	0.0706_{10}	0.6880_{196}	0.2420_{139}	0.862_{36}	-1.47_{23}	$5{,}578_{243}$
ℓ	0.0017_{21}	0.8451_{523}	0.1532_{419}	0.138_{36}	-25.12_{51}	80.43_{17}
$n_{10} = 0.075$, $n_{20} = 0.775$, $n_{30} = 0.150$						
g	0.0906_{30}	0.7468_{74}	0.1626_{54}	0.833_{28}	-1.60_{29}	$5{,}507_{222}$
ℓ	0.0053_{21}	0.9163_{267}	0.0784_{26}	0.167_{28}	-28.99_{49}	55.67_{103}
$n_{10} = 0.115$, $n_{20} = 0.800$, $n_{30} = 0.085$						
g	0.1355_{36}	0.7689_{63}	0.0956_{35}	0.843_{23}	-1.67_{22}	$5{,}530_{203}$
ℓ	0.0071_{23}	0.9580_{154}	0.0349_{15}	0.157_{23}	-29.46_{73}	52.06_{79}
$n_{10} = 0.150$, $n_{20} = 0.850$, $n_{30} = 0$						
g	0.2227_{124}	0.7773_{124}	0	0.665_{39}	-1.38_{20}	$5{,}614_{221}$
ℓ	0.0085_{22}	0.9915_{22}	0	0.335_{39}	-30.23_{48}	48.42_{88}

* n_{i0} is the initial overall mol fraction of species i, z_i is the mole fraction of species i in the vapor (g) or the liquid (ℓ) phase, ϕ is the molar fraction of a phase in the system, U^e is the excess internal energy (sum of the Lennard-Jones and Coulombic energies), and V_m is the molar volume. The simulation uncertainties are given in the last digits as subscripts.

both are slightly higher than the curve obtained from the UNIFAC + B-EOS approximation. We note that, in view of the poor results of the UNIFAC + B-EOS approximation for the liquid-phase composition of the methanol + MTBE binary system (Lísal et al., 1999b), the simulation and the Wilson + B-EOS for the liquid curve are likely more accurate overall. In contrast to the situation for the liquid curves, the simulation vapor curve agrees within its statistical uncertainties with the curve calculated from the UNIFAC + B-EOS approximation, and both are lower than obtained from the Wilson + B-EOS approximation. In this case, in view of the poor results of the Wilson + B-EOS approximation for the vapor-phase composition of the methanol + MTBE binary system (Lísal et al., 1999b), the simulation and the UNIFAC + B-EOS results for the vapor curve are likely more accurate overall. In view of the results for both curves, the VLE simulation results for the region near pure MTBE are better overall than either of the results based on thermodynamic models.

For the vapor–liquid region near the pure methanol, the simulation liquid compositions agree within their statistical uncertainties with those from the Wilson + B-EOS and UNIFAC + B-EOS approximations, and the simulation vapor compositions are lower than those from the Wilson + B-EOS and UNIFAC + B-EOS approximations. In view of the poor results of these approximations for the vapor composition of the methanol + isobutene binary system (Lísal et al., 1999b), the simulation results are to be preferred overall.

At $T = 360$ K, the vapor–liquid region occupies a large portion of the composition simplex. Comparing with Figure 2a, it is apparent that at lower temperatures the vapor–liquid region will move further toward the pure isobutene vertex and the liquid region will enlarge. The NPT RGEMC simula-

Table 5. Vapor–Liquid Equilibrium Data for the MTBE Ternary System at the Temperature 360 K and Pressure 5 Bar from the NPT RGEMC Simulations of this Article*

Isobutene (1) + Methanol (2) + MTBE (3); $T = 360$ K, $P = 5$ bar						
	z_1	z_2	z_3	ϕ	U^e (kJ/mol)	V_m (cm^3/mol)
$n_{10} = 0.270$, $n_{20} = 0.730$, $n_{30} = 0$						
g	0.5090_{207}	0.4910_{207}	0	0.512_{12}	-0.91_{7}	$5{,}660_{108}$
ℓ	0.0195_{166}	0.9805_{166}	0	0.488_{12}	-31.16_{49}	47.40_{96}
$n_{10} = 0.250$, $n_{20} = 0.650$, $n_{30} = 0.100$						
g	0.4278_{128}	0.4464_{172}	0.1257_{100}	0.557_{16}	-1.22_{18}	$5{,}408_{178}$
ℓ	0.0271_{59}	0.9018_{162}	0.0711_{129}	0.443_{43}	-30.09_{43}	54.25_{149}
$n_{10} = 0.225$, $n_{20} = 0.475$, $n_{30} = 0.300$						
g	0.3537_{114}	0.3737_{219}	0.2726_{178}	0.579_{21}	-0.95_{14}	$5{,}429_{180}$
ℓ	0.0522_{107}	0.6175_{289}	0.3303_{239}	0.421_{21}	-27.23_{59}	77.67_{259}
$n_{10} = 0.210$, $n_{20} = 0.300$, $n_{30} = 0.490$						
g	0.3182_{119}	0.2916_{194}	0.3902_{124}	0.568_{27}	-0.99_{19}	$5{,}398_{178}$
ℓ	0.0707_{90}	0.3126_{173}	0.6167_{149}	0.432_{27}	-24.98_{87}	102.2_{53}
$n_{10} = 0.250$, $n_{20} = 0.190$, $n_{30} = 0.560$						
g	0.3704_{150}	0.2209_{150}	0.4087_{189}	0.533_{38}	-0.85_{15}	$5{,}401_{144}$
ℓ	0.1131_{119}	0.1526_{192}	0.7343_{225}	0.467_{38}	-23.68_{37}	114.6_{18}
$n_{10} = 0.275$, $n_{20} = 0.125$, $n_{30} = 0.600$						
g	0.4314_{158}	0.1673_{100}	0.4013_{191}	0.457_{24}	-0.74_{11}	$5{,}410_{142}$
ℓ	0.1405_{109}	0.0889_{100}	0.7706_{171}	0.543_{24}	-23.23_{29}	119.2_{11}
$n_{10} = 0.315$, $n_{20} = 0.065$, $n_{30} = 0.620$						
g	0.4878_{166}	0.0944_{78}	0.4178_{199}	0.463_{29}	-0.70_{9}	$5{,}372_{118}$
ℓ	0.1647_{144}	0.0423_{59}	0.7930_{153}	0.537_{29}	-23.05_{37}	122.3_{11}
$n_{10} = 0.375$, $n_{20} = 0$, $n_{30} = 0.625$						
g	0.5501_{172}	0	0.4499_{172}	0.516_{34}	-0.70_{3}	$5{,}351_{122}$
ℓ	0.1883_{151}	0	0.8117_{151}	0.484_{34}	-22.87_{27}	125.1_{9}

*See Table 4 for notation.

Table 6. Vapor-Phase and Liquid-Phase Reaction Equilibrium Data for the MTBE Ternary System at the Temperature 360 K and Pressure 5 bar from the NPT REMC Simulations of this Article*

Isobutene (1) + Methanol (2) = MTBE (3); $T = 360$ K, $P = 5$ bar						
r		z_1	z_2	z_3	U^e (kJ/mol)	V_m (cm^3/mol)
0.337	g	0.044_{21}	0.6714_{7}	0.2846_{28}	-2.22_{34}	$5{,}152_{243}$
0.503	g	0.0752_{28}	0.5295_{14}	0.3953_{42}	-1.57_{24}	$5{,}209_{258}$
	ℓ	0.0319_{87}	0.5074_{44}	0.4607_{132}	-26.72_{51}	87.06_{144}
0.671	g	0.1193_{47}	0.4053_{32}	0.4754_{78}	-1.31_{16}	$5{,}413_{290}$
	ℓ	0.0475_{104}	0.3568_{70}	0.5957_{174}	-23.36_{39}	99.04_{14}
0.827	g	0.1687_{48}	0.3102_{39}	0.5211_{87}	-1.19_{25}	$5{,}318_{151}$
	ℓ	0.0753_{123}	0.2328_{102}	0.6919_{226}	-24.32_{43}	109.0_{16}
1.000	g	0.2280_{31}	0.2280_{31}	0.5440_{61}	-0.91_{12}	$5{,}353_{147}$
	ℓ	0.1119_{145}	0.1119_{145}	0.7762_{290}	-23.67_{35}	117.4_{15}
1.099	g	0.2661_{31}	0.1944_{34}	0.5395_{65}	-0.85_{9}	$5{,}372_{162}$
	ℓ	0.1574_{111}	0.0753_{122}	0.7673_{233}	-22.78_{49}	121.1_{22}
1.209	g	0.3066_{28}	0.1643_{34}	0.5291_{63}	-0.84_{12}	$5{,}321_{138}$
	ℓ	0.2088_{76}	0.0465_{91}	0.7447_{167}	-22.39_{35}	121.8_{12}
1.490	g	0.4021_{25}	0.1146_{36}	0.4833_{61}	-0.78_{9}	$5{,}383_{144}$
	ℓ	0.3388_{27}	0.0208_{40}	0.6404_{66}	-20.99_{36}	122.1_{16}
1.988	g	0.5274_{8}	0.0712_{15}	0.4014_{23}	-0.66_{4}	$5{,}396_{91}$
	ℓ	0.4957_{107}	0.0087_{15}	0.4956_{122}	-19.42_{38}	121.0_{19}
2.969	g	0.6702_{3}	0.0404_{10}	0.2894_{13}	-0.58_{3}	$5{,}456_{89}$

*r is the initial ratio of isobutene to methanol; for remaining notation, see Table 4.

tions and the prediction using the Wilson + B-EOS and UNIFAC + B-EOS approximations predict very similar shapes of the vapor–liquid region, and the vapor and liquid boundaries from all three methods differ only marginally. However, we note that, similar to the case of Figure 2b, in view of the better agreement with the underlying binary system composition (Lísal et al. 1999b), the simulation results are expected to be of slightly better accuracy overall.

Reacting MTBE ternary system

We considered the reaction and phase equilibria for the MTBE ternary system in two ways. First, we used the NPT REMC method to calculate the reaction equilibrium curves restricted to each of the gas and liquid phases at $T = 360$ K and $P = 5$ bar, as a function of the overall system composition. The intersections of these single-phase curves with the nonreacting ternary VLE surface yield a reactive VLE tie-line. Second, we used the NPT REMC method for the two-phase system at $P = 5$ bar and over a series of temperatures to directly calculate the reactive tie-line compositions at these (T, P) values.

Our single-phase reaction equilibrium simulation data are given in Table 6 and they are shown in Figure 3, together with our predictions of the single-phase reaction equilibrium using the B-EOS approximation in the gas phase and the Wilson and UNIFAC approximations in the liquid phase.

Figure 3 shows that both reaction equilibrium curves begin at the pure methanol vertex and end at the pure isobutene vertex, and the curves yield the single-phase reaction equilib-

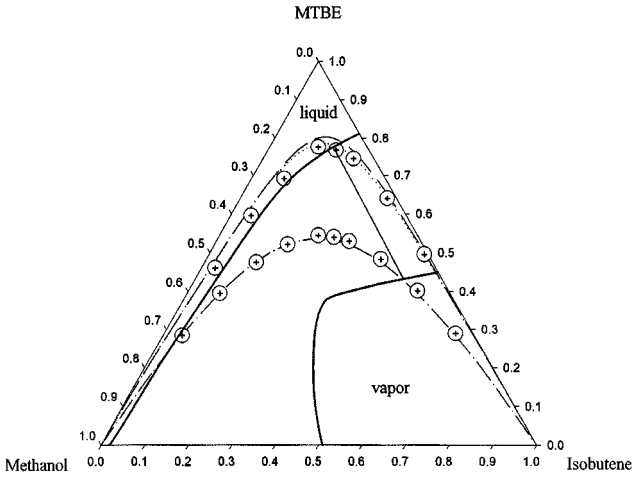

Figure 3. Triangular composition simplex for single-phase reaction equilibria in the MTBE ternary system at the temperature 360 K and the pressure 5 bar.

Crosses indicate the NPT REMC simulation results of this work, and circles around the crosses denote approximately the statistical uncertainties of the simulation results. The dashed and dotted lines represent our predictions of the liquid-phase reaction equilibrium using the Wilson and UNIFAC approximations, respectively, and the dot-dashed line is our prediction of the vapor-phase reaction equilibria using the B-EOS. Heavy solid lines indicate the nonreactive vapor–liquid region of Figure 2b. The light solid line connecting the intersections of the single-phase reaction-equilibrium curves with the vapor–liquid boundaries represents the reactive tie line.

rium composition, as the starting composition varies from pure methanol to pure isobutene. These single-phase reaction curves are thermodynamically unstable if they enter a nonreactive vapor–liquid region (our nonreactive vapor–liquid simulation region from Figure 2b is also plotted in Figure 3), or if they enter a single-phase region in which the opposite phase is more stable. Our vapor-phase reaction equilibrium simulations match the predictions using the B-EOS, as is to be expected (we also note that the vapor-phase reaction equilibrium results using the ideal-gas EOS differs only marginally from those obtained using the B-EOS). Our liquid-phase reaction equilibrium simulation results agree within their statistical uncertainties with the calculations obtained using the UNIFAC approximation, and they are slightly lower than the calculation using Wilson approximation. In contrast to the vapor-phase reaction-equilibrium curve, the liquid-phase reaction-equilibrium curve is slightly asymmetric (for example, the maximum is slightly higher than the stoichiometric value of 0.5); this fact is a consequence of the highly nonideal behavior of the MTBE reactive system in the liquid phase. We can also see from Figure 3 that many single-phase simulation points lie in the nonreactive vapor–liquid region, where they are thermodynamically unstable. However, we did not observe any peculiarities, for example, large fluctuations in the density or the composition during the simulations of these single-phase points. Finally, Ung and Doherty (1995c) observed a loop on a liquid-phase reaction equilibrium curve calculated by the Margules solution model; the loop was located in the nonreactive vapor–liquid region. Our liquid-phase reaction equilibrium curve, evaluated from the simulations and from the Wilson and UNIFAC approximations, did not show any loop.

At $T = 360\ K$ and $P = 5$ bar, the reactive tie-line is shown in Figure 3. This tie-line connects the intersection point of the liquid-phase reaction equilibrium curve with the nonreactive liquid boundary, and the intersection point of the vapor-phase reaction equilibrium curve with the nonreactive vapor boundary. The former is located at $\{x_1, x_2, x_3\} = \{0.146_{13}, 0.078_8, 0.776_{16}\}$ and the later at $\{y_1, y_2, y_3\} = \{0.480_{11}, 0.088_5, 0.432_{13}\}$; subscripts indicate uncertainties in the last digits. All the simulation points in the two-phase region in the figure are thermodynamically unstable (metastable).

We directly computed the reactive VLE tie-lines at the series of temperatures {370 K, 365 K, 362 K, 360 K, 355 K}, and $P = 5$ bar by means of NPT REMC simulations. These simulation results are listed in Table 7, and in Figure 4 they are compared with our results using the Wilson + B-EOS and UNIFAC + B-EOS approximations. We first note that at $T =$ 360 K and $P = 5$ bar, the directly simulated reaction and vapor–liquid equilibrium result agrees well with that determined indirectly from the results of Figure 3. The simulated compositions generally agree very well with the compositions predicted by the Wilson + B-EOS approximation. The compositions predicted by the UNIFAC + B-EOS approximation are also in good agreement with the simulations and with the Wilson + B-EOS compositions at T = 362 K, 360 K, and 355 K; they show disagreement at $T = 370$ K and 365 K.

Table 7. Vapor–Liquid and Reaction Equilibrium Data for the MTBE Ternary System at the Pressure 5 bar from the NPT REMC Simulations of this Article*

Isobutene (1) + Methanol (2) = MTBE (3); $P = 5$ bar						
	z_1	z_2	z_3	ϕ	U^e (kJ/mol)	V_m (cm_3/mol)
$T = 370$ K, $K = 1.0865$						
g	0.1189_{51}	0.5381_{114}	0.3430_{72}	0.832_{21}	-1.20_{16}	$5{,}592_{164}$
ℓ	0.0138_{37}	0.6878_{575}	0.2984_{563}	0.168_{30}	-27.20_{42}	44.26_{501}
$T = 365$ K, $K = 1.4615$						
g	0.2526_{101}	0.2571_{110}	0.4903_{61}	0.449_{51}	-0.86_{13}	$5{,}474_{134}$
ℓ	0.0682_{73}	0.1717_{131}	0.7601_{152}	0.551_{43}	-23.91_{35}	114.9_{14}
$T = 362$ K, $K = 1.7530$						
g	0.4019_{129}	0.1277_{76}	0.4704_{72}	0.524_{35}	-0.75_8	$5{,}428_{104}$
ℓ	0.1270_{139}	0.0608_{132}	0.8122_{196}	0.476_{29}	-23.30_{34}	122.0_{16}
$T = 360$ K, $K = 1.9823$						
g	0.4924_{123}	0.0822_{46}	0.4254_{85}	0.404_{21}	-0.70_5	$5{,}392_{100}$
ℓ	0.1682_{95}	0.0375_{68}	0.7943_{105}	0.596_{20}	-23.04_{27}	122.6_{10}
$T = 355$ K, $K = 2.7123$						
g	0.6133_{239}	0.0391_{43}	0.3476_{199}	0.398_{33}	-0.65_5	$5{,}328_{97}$
ℓ	0.2243_{141}	0.0162_{55}	0.7595_{155}	0.602_{29}	-22.69_{35}	122.4_8

*T is the temperature and K is the equilibrium constant given by Eqs. 10 and 14; for remaining notation, see Table 4.

Conclusions

We have performed REMC computer simulations for the isobutene + methanol + MTBE ternary system, both in the nonreacting case and in the case when equilibrium occurs for the reaction forming MTBE from the other two components. We incorporated within the REMC method our recently developed approach for phase equilibrium GEMC simulations called the RGEMC method (Lísal et al., 1999b). We modeled the system using an OPLS force-field model, and incorpo-

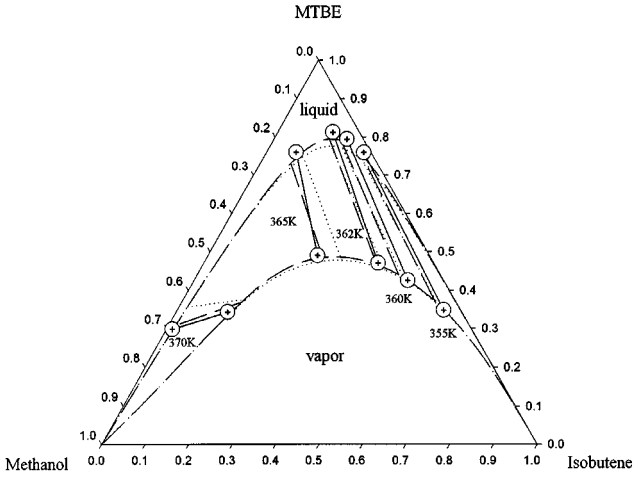

Figure 4. Projection in the ternary composition triangle of the complete reaction and phase-equilibrium diagram for the MTBE ternary system at the pressure 5 bar.

Crosses connected by solid lines indicate the reactive tie-lines at the series of temperatures {370 K, 365 K, 362 K, 360 K, 355 K}, as determined by the NPT REMC simulation results of this work; circles around the crosses denote approximately the statistical uncertainties of the simulation results. The dashed and dotted lines represent our predictions of the reaction and phase equilibrium using the Wilson + B-EOS and UNIFAC + B-EOS approximations, respectively.

rated no adjustable binary cross-interaction parameters. We studied the system at $P = 5$ bar and a range of temperatures, and compared our simulation results with those we calculated using conventional engineering approaches typified by the Wilson or the UNIFAC free-energy model for the liquid phase, accompanied by a truncated virial EOS for the gas phase. As is the case for the free-energy models, we used as input data the vapor-pressure curves of the pure substances. However, unlike the thermodynamic models, our simulations utilized no experimental mixture data of any kind.

No experimental data are available for this system, and its complexity makes it a severe test of simulation methodology and of thermodynamic models. We have found that our computer simulation results generally agree well with those calculated from the free-energy model approaches. However, we have also noted some discrepancies, and we have argued that the simulation results are likely of superior accuracy.

We believe that the results of this article show that the REMC method can be used to accurately predict combined reaction and phase equilibrium compositions for systems of experimental interest. It has advantages over conventional free-energy model approaches in that (1) less experimental data are required for its implementation; (2) it can also calculate excess internal energies and molar volumes as byproducts of the calculation; and (3) it requires no cross binary interaction parameters.

Acknowledgments

This research was supported by the Grant Agency of the Czech Republic under Grant 203/98/1446, by the Grant Agency of the Academy of Sciences of the Czech Republic under Grant A-4072712, and by the Natural Sciences and Engineering Research Council of Canada under Grant OGP1041.

Literature Cited

Allen, M. P., and D. J. Tildesley, *Computer Simulation of Liquids* Clarendon Press, Oxford (1987).

Barbosa, D., and M. F. Doherty, ''The Influence of Equilibrium Chemical Reactions on Vapor-Liquid Phase Diagrams,'' *Chem. Eng. Sci.*, **43**, 529 (1988).

Chase, M. W., C. A. Davies, and J. R. Downey, *JANAF Thermochemical Tables*, 3rd ed., *J. Phys. Chem. Ref. Data*, **14** (Suppl. 1) (1985).

Colombo, F., L. Cori, L. Dalloro, and P. Delogu, ''Equilibrium Constant for the Methyl *tert*-Butyl Ether Liquid-Phase Synthesis by Use of UNIFAC,'' *Ind. Eng. Chem. Fundam.*, **22**, 219 (1983).

DeGarmo, J. L., V. N. Parulekar, and V. Pinjala, ''Consider Reactive Distillation,'' *Chem. Eng. Prog.*, **43**, 43 (1992).

Doherty, M. F., and G. Buzad, ''Reactive Distillation by Design,'' *Trans. Inst. Chem. Eng.*, **70**, 448 (1992).

Frenkel, M., G. J. Kabo, K. N. Marsh, G. N. Roganov, and R. C. Wilhoit, *Thermodynamics of Organic Compounds in the Gas State*, TRC Data Series, Thermodynamic Research Center, College Station, TX (1994).

Jacobs, R., and R. Krishna, ''Multiple Solutions in Reactive Distillation for Methyl *tert*-Butyl Ether Synthesis,'' *Ind. Eng. Chem. Res.*, **32**, 1706 (1993).

Jedlovszky, P., and G. Pálinkás, ''Monte Carlo Simulation of Liquid Acetone with a Polarizable Molecular Model,'' *Mol. Phys.*, **84**, 217 (1995).

Lide, R. P., ed., *CRC Handbook of Chemistry and Physics*, CRC Press, Boca Raton, FL (1999).

Lísal, M., I. Nezbeda, and W. R. Smith, ''The Reaction Ensemble Method for the Computer Simulation of Chemical and Phase Equilibria: II. The $Br_2 + Cl_2 + BrCl$ System,'' *J. Chem. Phys.*, **110**, 8597 (1999a).

Lísal, M., W. R. Smith, and I. Nezbeda, ''Accurate Computer Simulation of Phase Equilibrium for Complex Fluid Mixtures. Application to Binaries Involving Isobutene, Methanol, Methyl *tert*-Butyl Ether, and *n*-Butane,'' *J. Phys. Chem. B*, 103, 10496 (1999b).

Marsh, K. N., P. Niamskul, J. Gmehling, and R. Bölts, ''Review of Thermophysical Property Measurements on Mixtures Containing MTBE, TAME, and Other Ethers with Non-Polar Solvents,'' *Fluid Phase Equilib.*, **156**, 207 (1999).

Marsh, K. N., ed., *API Project 44*, Thermodynamic Research Center, College Station, TX (1979).

Nezbeda, I., and J. Kolafa, ''The Use of Control Quantities in Computer Simulation Experiments: Application to the exp-6 Potential Fluid,'' *Mol. Simul.*, **14**, 153 (1995).

Panagiotopoulos, A. Z., ''Direct Determination of Fluid Phase Equilibria by Simulation in the Gibbs Ensemble: A Review,'' *Mol. Simul.*, **9**, 1 (1992).

Panagiotopoulos, A. Z., N. Quirke, M. Stapleton, and D. J. Tildesley, ''Phase Equilibria by Simulation in the Gibbs Ensemble. Alternative Derivation, Generalization and Application to Mixture and Membrane Equilibria,'' *Mol. Phys.*, **63**, 527 (1988).

Pedley, J. B., *Thermodynamical Data and Structures of Organic Compounds*, Vol. I, TRC Data Series, Thermodynamic Research Center, College Station, TX (1994).

Reid, R. C., J. M. Prausnitz, and B. E. Poling, *The Properties of Gases and Liquids*, 4th ed., McGraw-Hill, New York (1987).

Smith, J. M., H. C. Van Ness, and M. M. Abbott, *Introduction to Chemical Engineering Thermodynamics*, 5th ed., McGraw-Hill, New York (1996).

Smith, W. R., and R. W. Missen, ''Chemical Reaction Equilibrium Analysis: Theory and Algorithms,'' Wiley-Interscience: New York, 1982; reprinted with corrections, Krieger, Malabar, FL (1991).

Smith, W. R., and B. Tříska, ''The Reaction Ensemble Method for the Computer Simulation of Chemical and Phase Equilibria. I. Theory and Basic Examples,'' *J. Chem. Phys.*, **100**, 3019 (1994).

Ung, S., and M. F. Doherty, ''Vapor-Liquid Phase Equilibrium in Systems with Multiple Chemical Reactions,'' *Chem. Eng. Sci.*, **50**, 23 (1995a).

Ung, S., and M. F. Doherty, ''Calculation of Residue Curve Maps for Mixtures with Multiple Equilibrium Chemical Reactions,'' *Ind. Eng. Chem. Res.*, **34**, 3195 (1995b).

Ung, S., and M. F. Doherty, ''Theory of Phase Equilibria in Multireaction Systems,'' *Chem. Eng. Sci.*, **50**, 3201 (1995c).

Vetere, A., I. Miracca, and F. Cianci, ''Correlation and Prediction of the Vapor-Liquid Equilibria of the Binary and Ternary Systems Involved in MTBE Synthesis,'' *Fluid Phase Equilib.*, **90**, 189 (1993).

Vetere, A., ''The Prediction of Fluid Phase Equilibria of Subcritical Binary Systems by Using an Equation of State,'' *Fluid Phase Equilib.*, **64**, 107 (1991).

Walas, S. M., *Phase Equilibria in Chemical Engineering*, Butterworth, Boston (1985).

Wichterle, I., J. Linek, Z. Wágner, and H. V. Kehiaian, *Vapor-Liquid Equilibrium in Mixtures and Solutions*, ELDATA SARL, Paris (1996).

Appendix A: Wilson Free-Energy Model

The Wilson activity coefficients γ_i for the MTBE ternary system are given by (Ung and Doherty, 1995a):

$$\ln \gamma_i = 1 - \ln\left(\sum_{j=1}^{c} x_j \Lambda_{ij}\right) - \sum_{k=1}^{c}\left(\frac{x_k \Lambda_{ki}}{\sum_{j=1}^{c} x_j \Lambda_{kj}}\right),$$

where

$$\Lambda_{ij} = \frac{V_j}{V_i}\exp\left(-\frac{A_{ij}}{T}\right).$$

See Table A.1.

Appendix B: UNIFAC Free-Energy Model

The UNIFAC activity coefficients γ_i are given as the sum of a combinatorial part γ_i^C and a residual part γ_i^B (Reid et

Table A.1

Component	A_{ij} (K) Isobutene (1)	Methanol (2)	MTBE (3)	V (cm^3/mol)
Isobutene (1)	0	85.5447	−15.2212	93.33
Methanol (2)	1,296.7191	0	746.3971	44.44
MTBE (3)	136.6574	−204.5029	0	118.8

al., 1987):

$$\ln \gamma_i = \ln \gamma_i^C + \ln \gamma_i^R.$$

The combinatorial part γ_i^C is

$$\ln \gamma_i^C = \ln\left(\frac{\Phi_i}{x_i}\right) + 5q_i \ln\left(\frac{\Theta_i}{\Phi_i}\right) + l_i - \frac{\Phi_i}{x_i}\sum_{j=1}^{c} x_j l_j,$$

where

$$l_i = 4r_i - 5q_i + 1 \qquad \Theta_i = \frac{q_i x_i}{\sum_{j=1}^{c} q_j x_j} \qquad \Phi_i = \frac{r_i x_i}{\sum_{j=1}^{c} r_j x_j}$$

$$r_i = \sum_{k}^{\text{on }(i)} \nu_k^{(i)} R_k \qquad q_i = \sum_{k}^{\text{on }(i)} \nu_k^{(i)} Q_k.$$

Table B.1

Component	Group Identification Name	Main No.	Sec. No.	$\nu_j^{(i)}$	R_j	Q_j
Isobutene (1)	CH_3	1	1	2	0.9011	0.848
	$CH_2=C$	2	7	1	1.1173	0.988
Methanol (2)	CH_3OH	6	16	1	1.4311	1.432
MTBE (3)	CH_3	1	1	3	0.9011	0.848
	C	1	4	1	0.2195	0.0
	CH_3O	13	25	1	1.1450	1.088

Table B.2

Main No.	a_{mn} (K) 1	2	6	13
1	0	86.020	697.200	251.500
2	−35.360	0	787.600	214.500
6	16.510	−12.520	0	−180.600
13	83.360	26.510	339.700	0

The residual part γ_i^R is

$$\ln \gamma_i^R = \sum_{k}^{\text{on }(i)} \nu_k^{(i)} \left(\ln \Gamma_k - \ln \Gamma_k^{(i)}\right),$$

where

$$\ln \Gamma_k = Q_k\left[1 - \ln\left(\sum_m \Theta_m \Psi_{mk}\right) - \sum_m \left(\frac{\Theta_m \Psi_{km}}{\sum_n \Theta_n \Psi_{nm}}\right)\right]$$

$$\ln \Gamma_k^{(i)} = Q_k\left[1 - \ln\left(\sum_m^{\text{on }(i)} \Theta_m^{(i)} \Psi_{mk}\right) - \sum_m^{\text{on }(i)} \left(\frac{\Theta_m^{(i)} \Psi_{km}}{\sum_n^{\text{on }(i)} \Theta_n^{(i)} \Psi_{nm}}\right)\right]$$

$$\Theta_m = \frac{Q_m X_m}{\sum_n Q_n X_n},$$

where X_m is the mole fraction of group m in the mixture

$$\Psi_{mn} = \exp\left(-\frac{a_{mn}}{T}\right).$$

See Tables B.1 and B.2.

Manuscript received July 20, 1999, and revision received Nov. 16, 1999.